RuiZhi (Rebecca) Yu

On The Brink Of Chaos: Study Of Fermi-Pasta-Ulam Effects In 2D

Abstract

This work represents an extended computational study of the Fermi-Pasta-Ulam experiment for the dynamical nature of energy transfer among normal modes. A 2D lattice system with 40 particles is placed on a torus, where each particle is allowed to interact with its six nearest neighbors under the Lennard-Jones potential force law. Trajectories of the particles are analyzed through a Fourier transform method that calculates the amplitude and phase of each normal mode as a function of time. Results of the normal mode analyses and basic applications of the Lyapunov exponents show that Fermi-Pasta-Ulam effects are absent at small and large extremes of amplitude displacements. At an intermediate amplitude displacement, quasi-periodic behavior of the phase is seen initially and a secondary normal mode dominates the first one at irregular intervals. However, contrary to prediction, the system eventually reaches limited thermalization. This behavior resembles but is not characteristic of classical FPU effects.

I. Introduction

In 1955, an unpublished Los Alamos report simply titled, "Studies of Nonlinear Problems: I," began the first of a series of studies that would stimulate the current understanding of chaos theory and open the field of molecular dynamics simulation. In the Fermi-Pasta-Ulam (FPU) experiment, as it would later come to be known, researchers Enrico Fermi, John Pasta, and Stanislaw Ulam performed a normal mode analysis of a 64 particle chain on a vibrational string while the forces between the particles contained a non-linear term governed by either of the following two equations:

$$\ddot{x}_n = (x_{n+1} + x_{n-1} - 2x_n) + \alpha\left[(x_{n+1} - x_n)^2 + (x_n - x_{n-1})^2\right], \tag{1}$$

$$\ddot{x}_n = (x_{n+1} + x_{n-1} - 2x_n) + \beta\left[(x_{n+1} - x_n)^3 + (x_n - x_{n-1})^3\right], \tag{2}$$

where α and β represent the quadratic and cubic coefficients, respectively, and n=0, 1, 2,.., N-2, N-1 (N=64). Fixed end boundary conditions were included by considering $x_0 = x_n = 0$. [1,2]

According to the authors, *"The ergodic behavior of such systems was studied with the primary aim of establishing, experimentally, the rate of approach to the equipartition of energy among the various degrees of the system,"*[1] as they believed that through interactions with the quadratic and cubic terms of the equations, the system would experience thermalization. However, against their expectations, the system exhibited quasi-periodic behavior, where only a few low frequency normal modes gained any energy at all and particular normal modes alternated in dominating in energy at relatively regular periodic intervals. As they described, *"Instead of a gradual increase of all the higher modes, the energy is exchanged, essentially, among only a certain few."* [1,3]

Since then, the FPU experiment has, among others, led to solutions of integrable nonlinear equations such as the Korteweg-de Vries equations and consequently, advancements in soliton dynamics.[4] The FPU experiment has also opened new territory between chaos and order, as the results yield neither order nor chaos, but a combination of both. It has even been suggested that the results of the FPU experiment indicate that the theories of classical equilibrium statistical mechanics are no longer valid on a dynamical basis for systems at low temperatures.[5]

In the hope of attaining a better understanding, this study aims to expand the FPU experiment through modeling of a 2D lattice with the Lennard-Jones potential as forces. Furthermore, whereas Fermi, Pasta, and Ulam only calculated the amplitude of each normal mode, this study will calculate the phase of the corresponding normal mode as well. While the system is not expected to undergo thermalization, the energy is predicted to leak out of the initial normal mode more rapidly because of both the order of non-linearity of the Lennard-Jones potential and the 2D nature of the lattice, which allows for energy to flow in two directions instead of one. This is especially advantageous as the smaller quasi-periodic behavior will require shorter calculation times.

II. Models and Theory

II.1. The Lennard-Jones Potential

Trajectories of a 40 particle Lennard-Jones system are modeled using a computer code written in FORTRAN and compiled with the share software Cygwin Gnu FORTRAN compiler. The system obeys the Lennard-Jones force potential,

$$V_{LJ} = \varepsilon * \left(\frac{1}{r^{12}} - \frac{2}{r^6} \right),$$
(3)

where V_{lJ}, ε, and r represent the potential energy, the strength constant of the interaction, and the interspacing distance between two particles, respectively.
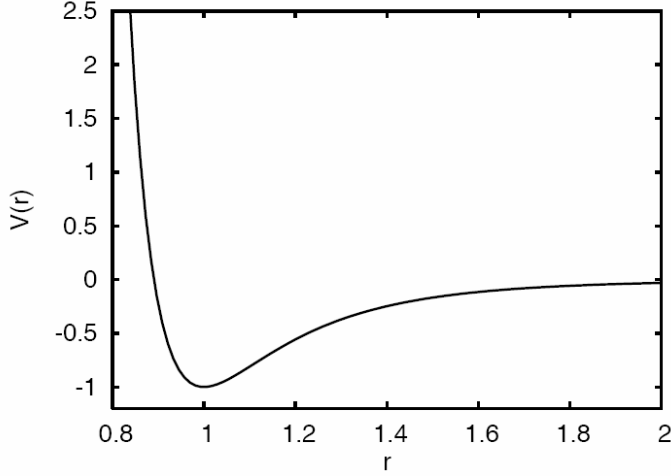
Figure 1: *The Lennard-Jones potential as a function of the interspacing distance. It gives $V(r)$ =- ε at its minimum.*

As shown in Fig. 1, the Lennard-Jones potential is characterized by a short range strongly repulsive core and a long range weakly attractive tail. The weak attraction of the tail models the van der Waals interaction whereas the strong core repulsion corresponds to the close range resistance of atoms to compression. While it was originally proposed for liquid argon, this potential has now been adapted to any pair of noble gas atoms i and j with interspacing distance r.[6] The negative derivative of the potential with respect to r yields the force,

$$F(r) = -\frac{dV}{dr} = 12\varepsilon * \left(\frac{1}{r^{13}} - \frac{1}{r^7} \right). \qquad (4)$$

II.2. Arrangement on 2D Torus Lattice

The atoms are placed on a lattice governed by two vectors $\vec{a_1}$ and $\vec{a_2}$ so that the position of each particle can be described by

$$R_n = n_1 \vec{a}_1 + n_2 \vec{a}_2, \tag{5}$$

where $n_1=0, 1, .., N_1-1$ and $n_2=0, 1, .., N_2-1$, as illustrated in Fig. 2a. To ensure periodic boundary conditions, the lattice is expanded to $R_n = n_1 \vec{a}_1 + n_2 \vec{a}_2$ where $n_1=-1, 0, ..., N_1-1, N_1$ and $n_2=-1, 0, ..,N_2-1, N_2$ to encompass a total of 70 particles (see Fig. 2b). The additional 30 particles are the virtual ones duplicated from those in the primary zone.
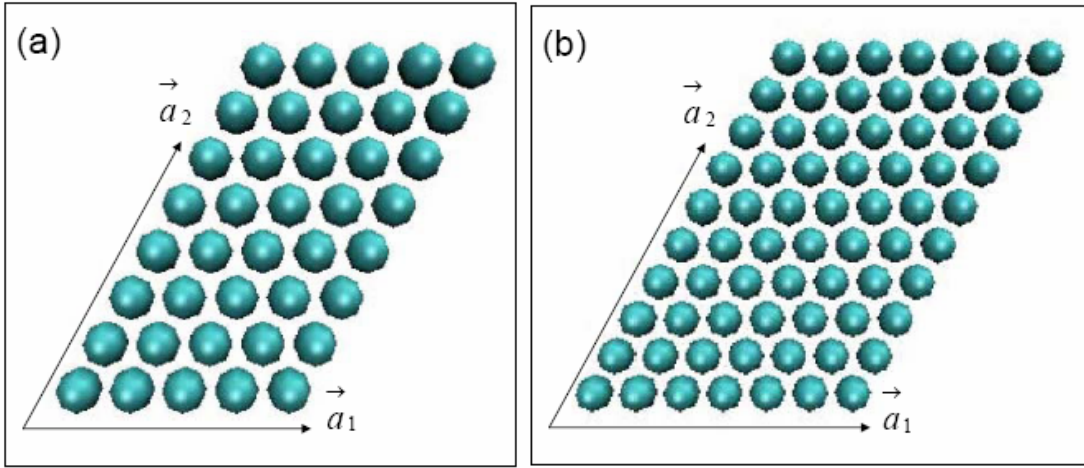
Figure 2: *Arrangement of atoms on a 2D lattice, where $N_1=5$ and $N_2=8$: (a) 5x8; and (b)7x10.*

However, while all 120 pair potentials are considered, an additional FORTRAN subroutine is utilized to arrange all interspacing distances in increasing order so that only nearest neighbor interactions are evaluated. That is, only the potentials and forces of the nearest six particles are calculated for each given particle. Since the interactions are not necessarily with the same six neighbors, this allows for the atoms to shift with some freedom, so that the system can not only model a solid but also a liquid. Nonetheless, under extremely large excitation energies, the lattice can begin to lose its structure and a sudden dislocation of an atom can result in an inaccuracy in force and energy calculations.

II.3. Displacement

In the beginning, each atom is assigned a particular displacement of a specific traveling wave normal mode regulated by the following two equations:

$$\vec{u}_i(t) = A_{k\lambda} \, \hat{\varepsilon}_{k\lambda} \cos\left(\vec{k} \cdot \vec{R}_i - \omega_{k\lambda} t + \phi_{k\lambda} \right), \tag{6}$$

$$\vec{v}_i(t) = A_{k\lambda} \, \hat{\varepsilon}_{k\lambda} \, \omega_{k\lambda} \sin\left(\vec{k} \cdot \vec{R}_i - \omega_{k\lambda} t + \phi_{k\lambda} \right), \tag{7}$$

where $\vec{u}_i$ and $\vec{v}_i$ are the position and velocity displacements of the ith particle, respectively. $A_{k\lambda}$ is the initial amplitude, t is the time, and $\phi_{k\lambda}$ is the corresponding initial phase, which is presumed to be 0 at $t=0$. $\omega_{k\lambda}$ and $\hat{\varepsilon}_{k\lambda}$ are the analogous frequencies and normalized eigenvector. $\vec{R}_i$ is the undisplaced position vector having the form $\begin{pmatrix} x_i \\ y_i \end{pmatrix}$. Finally, $\vec{k}$ is the related vector of the normal mode, as explained below.

Using a Fourier transform method similar to that used by Fermi, Pasta, and Ulam,[1] $\vec{u}_i$ is transformed from the real to the complex plane such that:

$$\vec{u}_i = \frac{1}{\sqrt{N}} \sum_k \vec{u}_k e^{i \vec{k} \cdot \vec{R}_n}, \tag{8}$$

where N equals to the number of particles and $k=1, 2, \ldots, N$. The k vector $\vec{k}$ is defined as $\vec{k} = \left(\dfrac{h_1 \vec{b}_1}{N_1} + \dfrac{h_2 \vec{b}_2}{N_2} \right)$ such that $\vec{a}_1 \cdot \vec{b}_1 = \vec{a}_2 \cdot \vec{b}_2 = 2\pi$ and $\vec{a}_1 \cdot \vec{b}_2 = \vec{a}_2 \cdot \vec{b}_1 = 0$. Then there exists a $K_{\alpha\beta}$ such that

$$K_{\alpha\beta} = 2\sum_{l\neq 0}\left[\left(v'(R_l)\delta_{\alpha\beta} + v''(R_l)R_{l\alpha}R_{l\beta}\right)\sin^2\left(\frac{\vec{k}\cdot\vec{R_l}}{2}\right)\right],\qquad(9)$$

where $\vec{R_l} = \vec{R_j} - \vec{R_i}$, the undisplaced position vector between particles j and i,

$v'(r) = \dfrac{1}{r}\dfrac{\partial V}{\partial r}$, and $v''(r) = \dfrac{1}{r}\dfrac{\partial}{\partial r}\left(\dfrac{1}{r}\dfrac{\partial V}{\partial r}\right)$.

For $\alpha = 1$, 2 and $\beta = 1$, 2, this yields a 2x2 real symmetric matrix of the form

$\begin{pmatrix} K_{xx} & K_{xy} \\ K_{xy} & K_{yy} \end{pmatrix}$. It can then be shown that

$$\sum_{\beta} K_{\alpha\beta}(k)\varepsilon_{\lambda\beta}(k) = M\omega_\lambda^2(k)\varepsilon_{\lambda\alpha}(k),\qquad(10)$$

where $\varepsilon_{\lambda\beta}(k)$ is the eigenvector and $M\omega_\lambda^2(k)$ is the eigenvalue. In this case, since the

mass M is arbitrarily chosen to be one Lennard-Jones unit, the eigenvalue is simply the

square of the frequency.

An adapted FORTRAN code[8] is used to diagonalize the matrices for the

eigenvectors and eigenvalues.

II.4. Propagation of System

The system is propagated with the Verlet algorithm,[9,10] which exploits the

positions and forces of the two previous steps to predict the trajectory of the next step as

$$x(t + \Delta t) = 2x(t) - x(t - \Delta t) + \frac{1}{M}F[x(t)]\Delta t^2.\qquad(11)$$

At time t=0, the previous step $x(t - \Delta t)$ is calculated by the Taylor expansion of

$x(t - \Delta t)$ around the center t=0. The trajectories are then converted into movie

simulations using the shareware, Visualizing Molecular Dynamics (VMD).[7]

Equations (6) and (7) are written into more comprehensive forms, which are the most general solutions of Newton's laws for harmonic oscillators:

$$\vec{u}_i(t) = \text{Re} \sum_{k\lambda} A_{k\lambda} \,\hat{\varepsilon}_\lambda(k) e^{i\left[\vec{k}\bullet\vec{R}_i - \omega_\lambda(k)t + \phi_{k\lambda}\right]}, \tag{12}$$

$$\vec{v}_i(t) = \text{Re} \sum_{k\lambda} -i\omega_\lambda(k) A_{k\lambda} \,\hat{\varepsilon}_\lambda(k) e^{i\left[\vec{k}\bullet\vec{R}_i - \omega_\lambda(k)t + \phi_{k\lambda}\right]}. \tag{13}$$

Consequently, these equations are inverted using the relation $\dfrac{1}{N}\sum_i e^{i(\vec{k}-\vec{k}')\bullet R_i} = \delta_{kk'}$ and

$\sum_\alpha \varepsilon_{\lambda\alpha}(k)\varepsilon'_{\lambda\alpha}(-k) = \delta_{\lambda\lambda'}$ for eigenvectors. Solving the equations yields

$$A_{k\lambda}(t)e^{i(\phi_{k\lambda}-\omega_{k\lambda}t)} = \frac{1}{N}\sum_i^N \left(\vec{u}_i(t) + i\frac{\vec{v}_i(t)}{\omega_{k\lambda}}\right) \bullet \hat{\varepsilon}_{k\lambda}\, e^{(-i\vec{k}\bullet\vec{R}_i)} \tag{14}$$

for the determination of amplitude and phase of a particular normal mode at the time t.

II.5. Calculation of Amplitude and Phase for Corresponding Normal Modes

In the trajectory FORTRAN program, the displacements $\vec{u}_i$ are calculated separately and written into a data file. A separate code is utilized to read in the data and map the amplitude and phase.

For a complex number $F = A_{k\lambda}(t)e^{i(\phi_{k\lambda}-\omega_{k\lambda}t)}$, $|F| = \left|F\cdot F^*\right|^{\frac{1}{2}}$, where F^* is the complex conjugate of F. Thus, $A_{k\lambda}(t)$ is simply the square root of the sum of the squares of the real and imaginary components of F. The phase $\phi_{k\lambda}$ is calculated through the amplitude. $\eta_{k\lambda}(t)$ is determined from the normal mode corresponding to a particular value of k and λ. Since $\eta_{k\lambda}(t)$ is a complex number for a given time t, it can assume the

form $\eta_{k\lambda}(t) = \eta^r_{k\lambda}(t) + i\eta^i_{k\lambda}(t)$, where $\eta^r_{k\lambda}(t)$ is the real component and $\eta^i_{k\lambda}(t)$ the corresponding imaginary one. A second variable is defined as

$$\xi_{k\lambda}(t) = \xi^r_{k\lambda}(t) + i\xi^i_{k\lambda}(t) = e^{i\omega_{k\lambda}t}\eta^{k\lambda}(t) = e^{i\omega_{k\lambda}t}A_{k\lambda}(t)e^{i(\phi_{k\lambda}-\omega_{k\lambda}t)} = A_{k\lambda}(t)e^{i\phi_{k\lambda}}. \quad (15).$$

Consequently, we have

$$\cos\phi_{k\lambda}(t) = \frac{\xi^r_{k\lambda}(t)}{A_{k\lambda}(t)} \qquad (16)$$

and

$$\sin\phi_{k\lambda}(t) = \frac{\xi^i_{k\lambda}(t)}{A_{k\lambda}(t)}, \qquad (17)$$

which yield sufficient information for the calculation of the phase.

All calculations are carried out on a 1.7GHz Personal Laptop, and require approximately three hours for every set of a million of data points. Moreover, instead of plotting the particular energy of a normal mode, the amplitude of the normal mode is graphed. However, the energy is easily calculated by $E_{k\lambda} = \frac{(A_{k\lambda}\omega_{k\lambda})^2}{2}$. Finally, the Δt used for the propagation process is 0.01. In some cases, data are recorded for only every 100 points to save disk space.

II.6. The Lyapunov Exponent

The separation of two trajectories is defined as:

$$d(t) = \sqrt{\left\|\vec{u}_1(t) - \vec{u}_2(t)\right\|^2 + \frac{\left\|\vec{p}_1(t) - \vec{p}_2(t)\right\|^2}{m^2\omega^2}}, \qquad (18)$$

where u is the displacement, p the momentum, and m and ω the mass and frequency of oscillation, respectively. The largest Lyapunov exponent is $d(t) \approx ce^{\lambda t}$ for some constant

9

c and Lyapunov exponent λ. For a N-dimensional phase space, there are N Lyapunov exponents, the largest of which describes the extent of chaos of the system. In fact, a Lyapunov exponent $\lambda \prec 0$ describes a non-conservative, dissipative system such as a damped harmonic oscillator. A Lyapunov exponent $\lambda = 0$ indicates a conservative non-chaotic system, such as that of a simple harmonic oscillator. Finally, $\lambda \succ 0$ indicates a chaotic, unstable system.[11,12] In this study, the presence or absence of the nonzero Lyapunov exponent is used to establish the degree of chaos of a system.

III. Numerical Simulation and Discussion

III.1.Verification of FORTRAN Code

In order to confirm the accuracy of the aforementioned methods and the efficiency of the coding, the program is operated under certain test conditions. First, the simulated system is shown to exhibit conservation of total energy, which is described by $E_T = \sum_{i=1}^{n}(PE(i) + KE(i))$, the sum of the potential and kinetic energies of the particle. For each run for the calculation of the trajectory of the system, the root mean square (rms) error is calculated by $E_{rms} = \left[\dfrac{1}{n} \sum_{i=1}^{n} \left[\dfrac{E_T}{n} - \left(PE(i) + KE(i)\right) \right]^2 \right]^{1/2}$. For harmonic and near harmonic systems, this value is approximately 1.5×10^{-6}. For systems with larger amplitude displacements, it increases to approximately 3×10^{-3}, which is still a reasonable computational error.

Of course, conservation of energy does not guarantee an accurate code. The trajectory of the system is also viewed through the VMD movie simulator and

qualitatively confirmed to exhibit the propagation of a traveling wave at small amplitude displacements, as expected.

As a further verification, the force potential is altered to the harmonic potential $V_H(r) = 36(r-1)^2 - 1$ and assigned an initial amplitude displacement $A_{(13,1)} = 0.05$, where (13, 1) indicates a particular normal mode. Using a random number generator subroutine, the initial positions and velocities of the particles are given another arbitrary displacement. A normal mode analysis, shown in Fig. 3, confirms that the amplitudes and phases stay constant, also as expected.
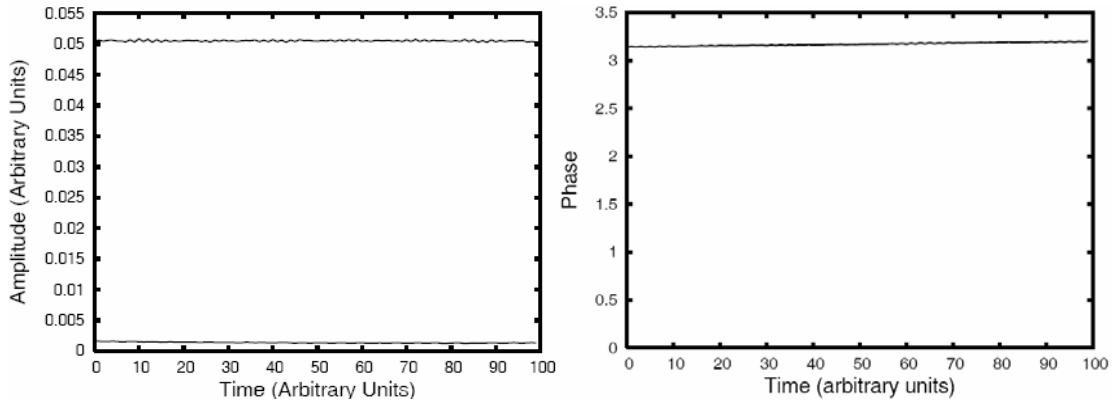
Figure 3: *The amplitudes of two normal modes (left panel) and the phase of one normal mode (right panel) are constant, indicating that in a harmonic system, no energy leaks out of the normal mode. Note: Slight fluctuations in the lines are results of trivial numerical errors generated by the program.*

III.2. Nearly Harmonic Behavior

Due to the nearly parabolic behavior of the Lennard-Jones potential at small amplitude displacements, *e.g.*, for $A_{k\lambda} = 0.01$, the system is well-behaved, with only minor deviations from the trajectory of a perfectly harmonic oscillator. This is supported by the system exhibiting a $\lambda = 0$, as shown in Fig. 4, where the separation is the distance between a trajectory with a perfectly harmonic displacement of 0.01 LJ units and another trajectory with initial displacement determined by a FORTRAN subroutine that specifies

small, random deviations less than 0.1% of the original deviation. In this case, the corresponding projection indicates that almost all energy, which has a direct relationship with the amplitude displacement, is retained in original normal mode, as shown in Fig. 5.
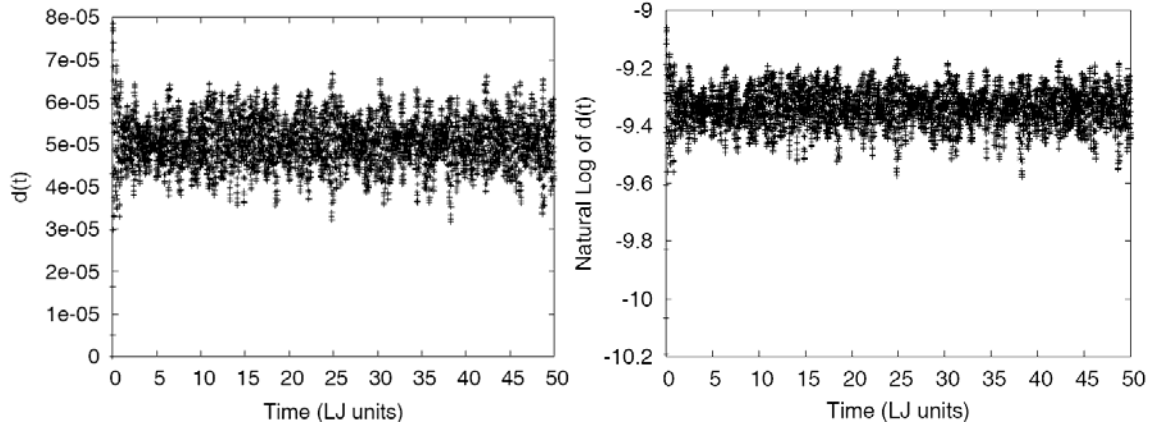
Figure 4: Separation of two trajectories with initial displacement of approximately 0.01 LJ units: The separation as a function of time (in the left panel); and the natural log (ln) of separation as a function of time (in the right panel). The linear behavior with zero slope (constant behavior) of both functions indicates a complete lack of chaotic behavior.
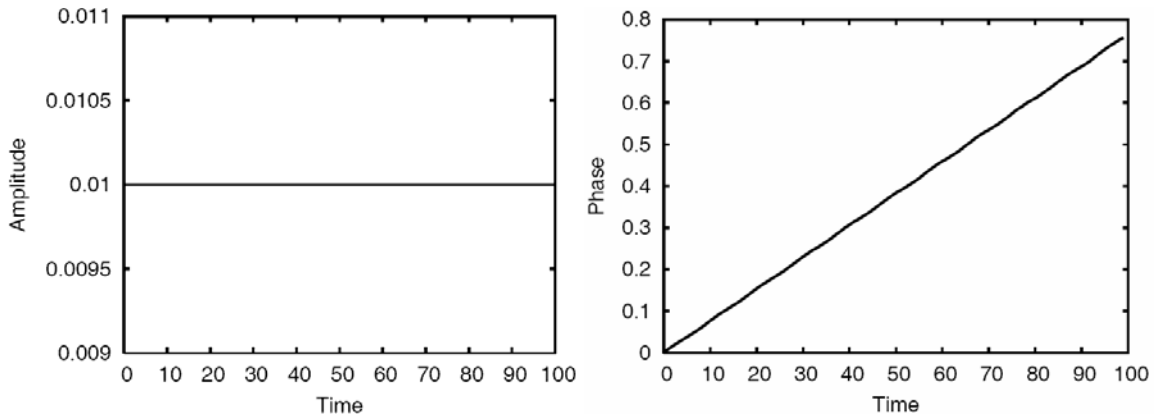

Figure 5: The amplitude (left) and phase (right) of a particular normal mode, where the amplitude remains at 0.01 for over 20 cycles and the phase is a simple linear evolution through time.

III.3 Chaotic Behavior

On the other hand, if the system is infused with excessive energy, the non-linear forces of the Lennard-Jones potential will dominate, and the trajectories will deviate significantly from that of the perfectly harmonic oscillator. When assigned an amplitude

displacement of $A_{(13,1)} = 0.1$, the system does not yet break, but is already exhibiting

chaotic behavior, as shown in Fig. 6.
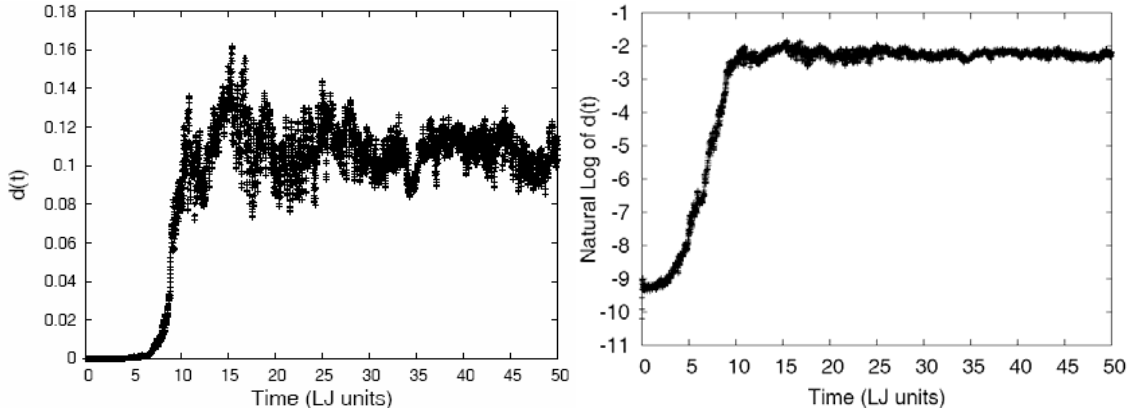
Figure 6: Separation of two trajectories with initial displacement of approximately 0.1 LJ units. The separation as a function of time is shown in the left panel. The natural log (ln) of separation as a function of time is given in the right panel. The exponential growth demonstrated in d(t) is confirmed by the linear behavior of its logarithm, whose positive slope between approximately 5 and 10 LJ units indicates a chaotic system.
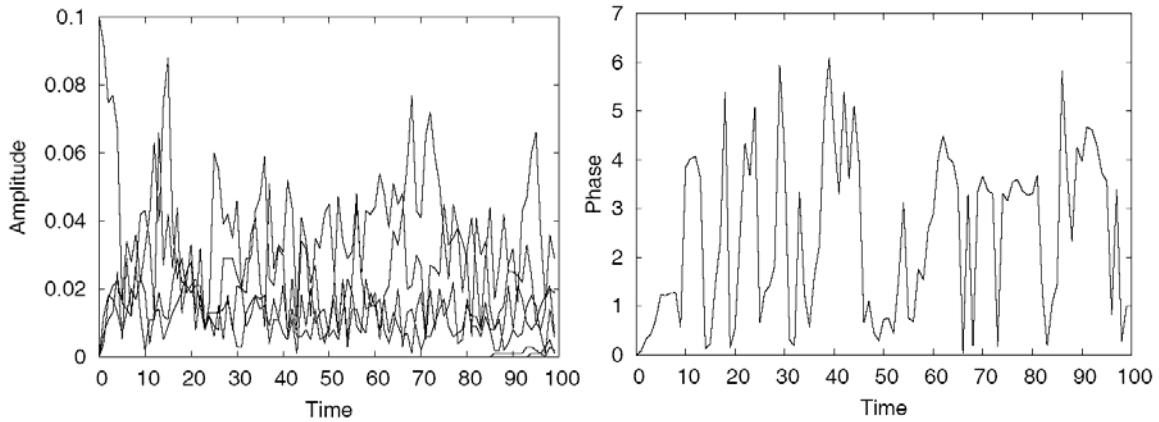
Figure 7: The normal mode analysis for $A_{(13,1)} = 0.1$: In the left panel, a limited thermalization occurs for a selected number of normal modes as the amplitude of the original normal mode decreases and that of six others slightly increase. However, contrary to typical Fermi-Pasta-Ulam effects, no normal mode other than the original one dominates at any particular time. The phase of the original normal mode over time is shown in the right panel.

However, it is interesting that the positive Lyapunov exponent is not apparent

until after approximately the first period ($\omega \approx 4.59$ for this particular normal mode) and

saturates after approximately two periods. It is hypothesized that the extent of this maximum separation is limited by the potential force law and the kinetic and potential energy distributions in such a manner that further separation would break the system.

An analysis of the normal modes is, in a way, surprising (see Fig. 7). The system does not break, as limited thermalization does occur in selected normal modes. Moreover, to some extent, the amplitude displacement curves exhibit some amplitude modulation and are not completely smooth. This may result from a rapid leaking of energy out of the original normal mode due to the 2D lattice structure permitting for interaction with six nearest neighbors and the non-linear behavior of the Lennard-Jones potential. Both these factors account for a faster rate of thermalization than that of the FPU experiment.

III.4. On the Brink of Chaos

Above all, this research is interested in the region where order and chaos blend, as demonstrated in Fig. 8. With a slightly smaller amplitude of $A_{(13,1)} = 0.07$, the onset of the Lyapunov exponent is less visible and is not fully apparent until after 25 LJ units of time, over 5 cycles later. Furthermore, the slope of the natural logarithm graph is smaller than that of the previous one, indicating a smaller Lyapunov exponent and thus, less chaos.

The corresponding normal mode analysis, shown in Fig. 9, indicates that the energy does not rapidly leak out of the original normal mode as it did for the partially thermalized system. However, the modulation of amplitude still persists. Yet, remarkably, eventual limited thermalization does occur as the amplitude of the original normal mode decreases and settles to approximately 0.02. Moreover, unlike that of the chaotic system, the original normal mode does not always dominate; at times it is supplanted by a second normal mode, which gains energy at 100 LJ units before losing it

after approximately 300 LJ units. This normal mode also settles at an amplitude of approximately 0.02.
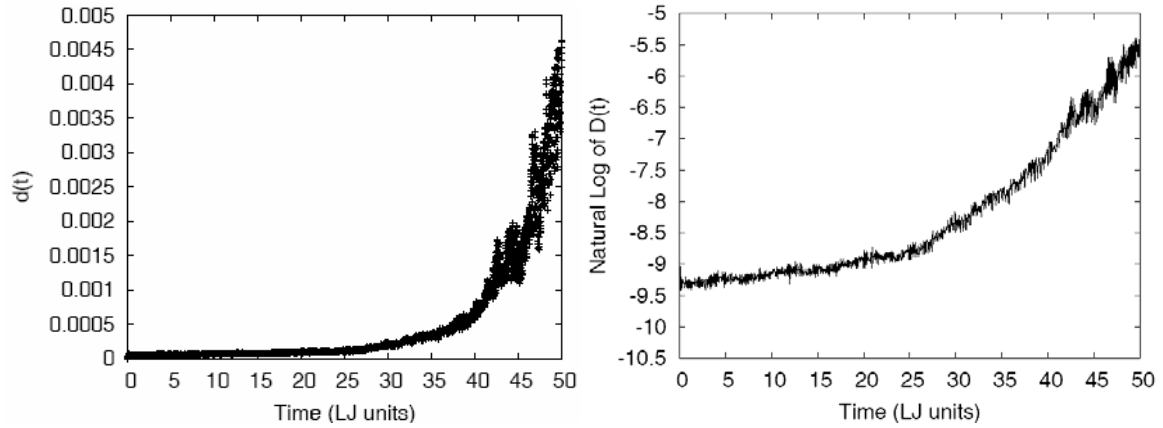
Figure 8: *Separation of two trajectories with initial displacement of approximately 0.07 LJ units: The separation as a function of time is given in the left panel and the natural log (ln) of separation as a function of time is shown in the right panel.*
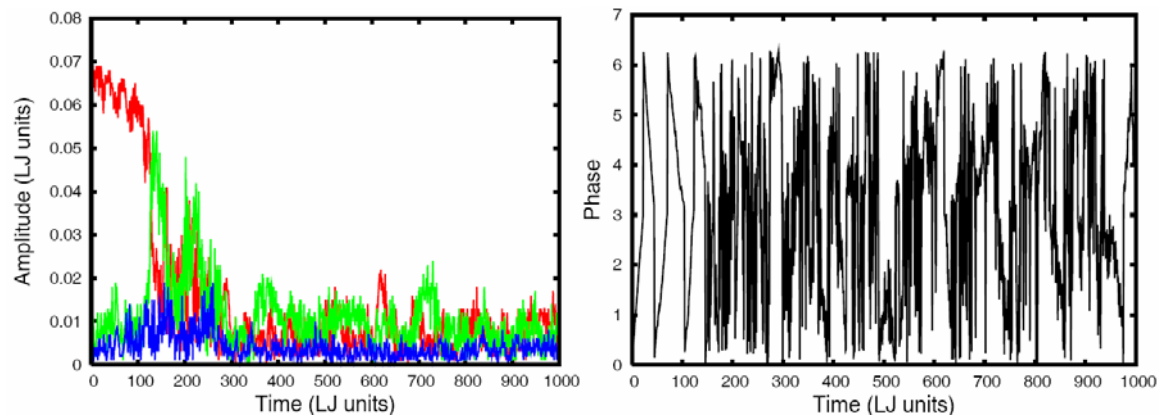
Figure 9: *The normal mode analysis (amplitudes in the left panel, and phase in the right one) for $A_{(13,1)} = 0.07$. The amplitude is displayed for three particularly interesting normal modes, but the phase is shown for only the original normal mode. Note that it is not merely in these three modes in which the energy of the system is transferred.*

Most interestingly, the phase of the original normal mode initially exhibits quasi-periodic behavior as it gradually shifts upwards and downwards again, which parallels the results produced by Fermi, Pasta, and Ulam for their normal mode analysis of the amplitudes and energies. This behavior is disrupted at approximately 150 LJ units, which

corresponds to the time when original normal mode has reached its estimated final amplitude.
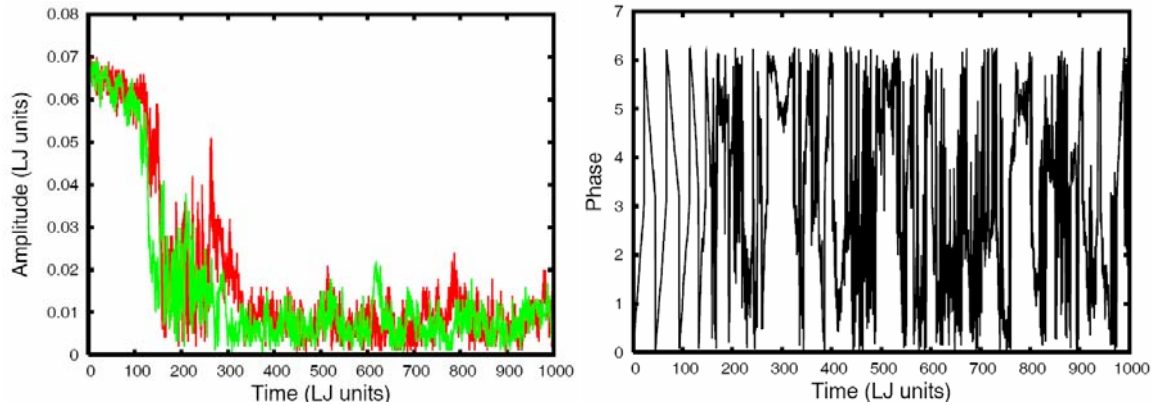
Figure 10: *The amplitude of the original normal mode for Δt=0.01 and Δt= 0.005 (left) and the phase for the original normal mode with Δt =0.005 (right).*

In order to verify the results, the system is given the same conditions with a different time step to ensure that they are not a result of a numerical error (see Fig. 10). The graph above indicates that while there are quantitative differences in the data, the qualitative result is the same. Furthermore, with a reduced time step, the phase of the original normal mode still exhibits quasi-periodic behavior until 150 LJ units, as before. Since numerical computations always exhibit some error due to rounding and some inaccuracy of integrating algorithms, this is acceptable.

Finally, the possibility of whether $A_{(13,1)} = 0.07$ is too closely associated with chaos is addressed. The amplitude is decreased to 0.056, which is the value, to the nearest thousandth, where the first visible indications of non-harmonic behavior begin. Since the smaller amplitude also yields smaller numerical errors, this is also another method to verify the accuracy of the results for the larger amplitude.

The results in Fig. 11 parallel that of Fig. 10. It takes a longer time for the energy to leak out of the original normal mode, which is expected for smaller amplitudes.

Furthermore, it is interesting to note that as before, the phase exhibits quasi-periodic behavior while the amplitude remains at approximately 0.056.
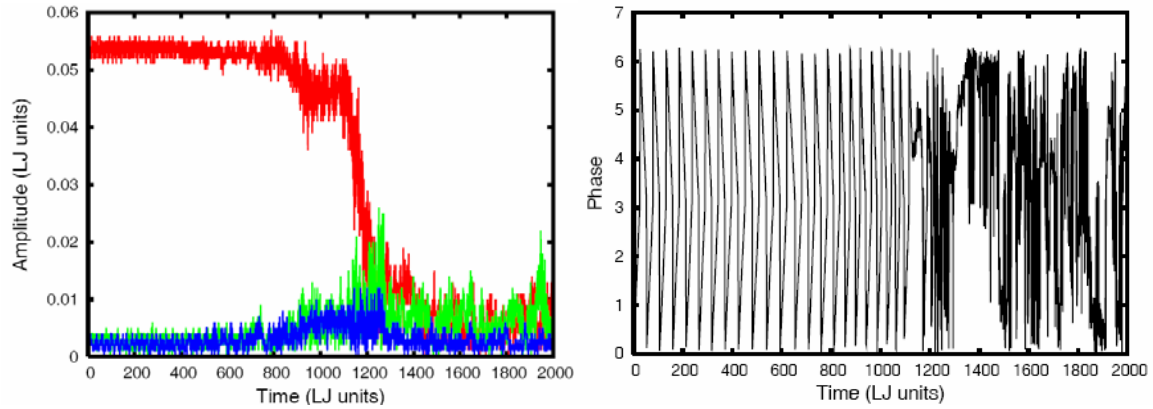
Figure 11: *The normal mode analysis for* $A_{(13,1)} = 0.056$. *The amplitudes of three interesting normal modes (left) and the phase of the original (right) are shown.*

There are several explanations for this lack of traditional Fermi-Pasta-Ulam results. First, as mentioned in the hypothesis, the rapid flow of energy due to an added dimension to the system may account for the limited thermalization before FPU effects can set in. Moreover, although similar lattices and conditions have been studied, this exact system has never been employed. For instance, when the Lennard Jones potential is altered to the power law potential of Fermi, Pasta, and Ulam described by $V_{PP}(r) = 36(r-1)^2 - 252(r-1)^3 - 1$, the system breaks with $A_{(13,1)}$ approximately greater than 0.05. Thus, these results may also result from the high degree of the Lennard Jones potential equation.

Finally, there does not exist a proven theory that states FPU effects must occur. The Kolmogorov–Arnold–Moser (KAM) theorem that emerged out of the dynamical simulations in the 1950s, which is the closest proof for its existence, is merely an explanation for the FPU effects and does not explicitly state the conditions under which they occur.

IV. Conclusions

This work has performed a systematical study of the regular and chaotic character of a 2D Lennard-Jones model using a molecular dynamics approach. Results are analyzed in terms of the Lyapunov exponent and the Fourier transform normal mode analysis methods. Since the Lennard-Jones potential is analogous to that of a harmonic, parabolic potential, there is no chaos for small amplitude displacements, such as $A_{k\lambda} = 0.01$. On the other hand, a large amplitude displacement $A_{k\lambda} = 0.1$ indicates a chaotic system with a large, positive Lyapunov exponent and limited thermalization.

Finally, for a system with $A_{k\lambda} = 0.07$ that is "on the brink of chaos," the normal mode analysis indicates astonishing results. Rather than exhibiting FPU effects as predicted, the system undergoes limited thermalization much like that of the chaotic system. Unlike the chaotic system, a secondary normal mode dominates the original normal mode at certain intervals, which is characteristic of the FPU graphs. However, there does not appear to be any regular pattern concerning these intervals. Furthermore, quasi-periodic behavior of the phase is also observed while most of the energy is in the original normal mode, suggesting that Fermi-Pasta-Ulam effects do not apply to energy only. Nonetheless, this behavior is lost with the onset of limited thermalization.

VI. Future Work

Since these results are astounding and unexpected, further work will provide a better argument for their accuracy. The Verlet algorithm is an efficient propagation method, but its accuracy has limitations. During this research, a predictor-corrector integration method had also been used for propagation and yielded similar results. However, since error accumulation is always a source of worry for numerical

RuiZhi (Rebecca) Yu

calculations, the system should be propagated with a third or maybe, fourth method for confirmation.

Moreover, this research only gives an initial amplitude displacement to one particular normal mode of the lowest non-zero frequency. There also exists another normal mode with the same frequency. This normal mode and others of similar low frequencies should be given initial displacements. The results should be comparable.

Finally, since these results indicate an astounding deviation from the traditional FPU experiments, they suggest that further exploration as to precisely why they occur is required. Although the 2D nature of the lattice and the Lennard Jones potential force law account for some rapid leaking of energy between normal modes, they do not fully explain the limited thermalization that occurs, even for systems with intermediate amplitude displacements. As a further confirmation, the lattice should be reduce to 1D and tested with different force laws. Despite all unexpected results, this research undoubtedly provides a novel opportunity for future investigations.

VII. Acknowledgments

References

[1] E. Fermi, J. Pasta, and S. Ulam, "Studies of nolinear problems," Los Alamos document LA-1940 (1955).

[2] G.M. Zaslavsky, "Long way from the FPU-problem to chaos," *Chaos*, **15**(1), 015103 (2005).

[3] L. Galgani and A. Giorgilli, "Recent Results on the Fermi-Pasta-Ulam Problem," *Journal of Mathmatical Sciences,* **128**(2), 2761 (2005).

[4] T.P. Weissert, *The Genesis Of Simulation In Dynamics Pursuing the Fermi-Pasta-Ulam Problem,* New York: Springer-Verlag New York Inc, 1997.

[5] A. Carati, L.Galgani, and A. Giorgilli, "The Fermi-Pasta-Ulam problem as a challenge for the foundations of physics," *Chaos,* **15**(1), 015105 (2005).

[6] D.C. Rapaport, *The Art of Molecular Dynamics Simulation*, Cambridge: Cambridge University Press, 1996.

[7] W. Humphrey, A. Dalke, and K. Schulten, "VMD-Visual Molecular Dynamics" *J.Molec. Graphics,* **14**(1), 33 (1996).

[8] W.H. Press, P.B. Flannery, S.A. Teukolsky, and W.T. Vetterling, *Numerical Recipes in FORTRAN.* Cambridge: Cambridge Unversity Press, 1992.

[9] L.Verlet, "Computer experiments on classical fluids.I. Thermodynamical properties of Lennard-Jones molecules," *Phys. Rev,* **159**, 98 (1967).

[10] L Verlet, "Computer experiments on classical fluids. II. Equilibrium correlation functions," *Phys. Rev,* **165**, 201 (1968).

[11] G.L. Baker and J.P. Gollub, *Chaotic Dynamics An Introduction*, Cambridge: Cambridge University Press, 1990.

[12] D.J. Evans and G.P. Morris, *Statistical Mechanics of Nonequilibrium Liquids*, London: Academic Press, 1990.